

LECTURE 11: FEIGENBAUM'S ANALYSIS OF PERIOD DOUBLING, SUPERSTABILITY OF FIXED POINTS AND PERIOD-P POINTS, RENORMALISATION, UNIVERSAL LIMITING FUNCTION, DISCRETE-TIME DYNAMICS ANALYSIS METHODS, THE POINCARÉ SECTION, THE POINCARÉ MAP, THE LORENZ SECTION, ATTRACTOR RECONSTRUCTION

Contents

1	Feigenbaum's analysis of period doubling	2
1.1	The Feigenbaum constants	2
1.2	Superstable fixed points and period-p points	2
1.3	Renormalisation and the Feigenbaum constants	5
1.4	Numerical determination of the Feigenbaum α constant	8
2	Discrete-time analysis methods	9
2.1	The Poincaré section and the Poincaré map	9
2.1.1	Example of finding a Poincaré map formula	10
2.2	The Poincaré analysis of the periodically driven damped Duffing oscillator	11
2.3	The Poincaré analysis of the Rössler attractor	14
3	The Lorenz section of 3-D attractors	15
4	Attractor reconstruction	16

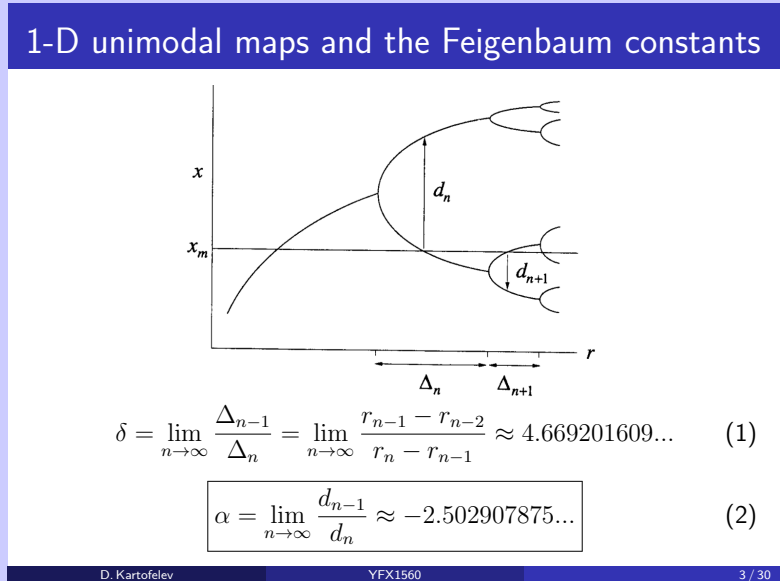
1 Feigenbaum's analysis of period doubling

In this lecture we are continuing our study of one-dimensional maps as simplified models of chaos and as tools for analysing higher order differential equations. We have already encountered maps in this role. The Lorenz map provided strong evidence that the Lorenz attractor is truly chaotic or in other words strange, and is not just a long-period limit-cycle, see Lectures 9 and 10.

1.1 The Feigenbaum constants

The Feigenbaum constants were presented during Lecture 10.

SLIDE: 3



In the above orbit diagram $x_m = \max f(x)$ is the maximum of the unimodal map graph. The **Feigenbaum constants** are valid up to the onset of chaos at the accumulation point $r = r_\infty$ and inside each **periodic window** for $r > r_\infty$. The **Feigenbaum constants** are **universal** the same convergence rate appears no matter what unimodal map is iterated! For us they are **new mathematical constants**, as **basic to period doubling** as π is to circles.

Showing the values of the Feigenbaum constants to 30 decimal places:

$$\delta = 4.669\,201\,609\,102\,990\,671\,853\,203\,821\,578, \quad (1)$$

$$\alpha = -2.502\,907\,875\,095\,892\,822\,283\,902\,873\,218. \quad (2)$$

In this lecture we'll take a closer look at the Feigenbaum α constant. We show how it was derived.

1.2 Superstable fixed points and period-p points

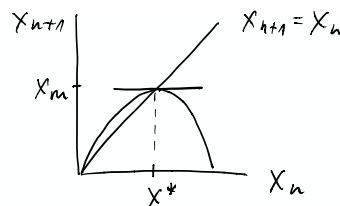


Figure 1: Superstable fixed point where $f'(x^*) = 0$ and at the same time $x^* = x_m$ where x_m is the maximum of given map function f .

The fixed point defined by

$$f(x^*) = x^*, \quad (3)$$

is said to be **superstable** if its slope

$$f'(x^*) = 0. \quad (4)$$

This holds true when the maximum (or minimum) of map function f happens to also be the fixed point

$$x^* = x_m = \max f(x), \quad (5)$$

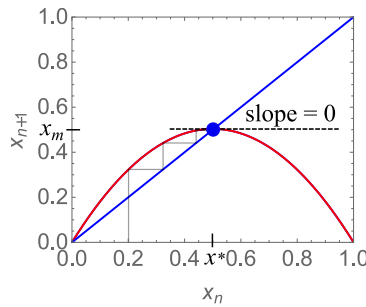
where x_m denotes the maximum. Figures 1, 2 and Slide 4 show the superstable fixed point of the unimodal logistic map given by

$$x_{n+1} = rx_n(1 - x_n), \quad (6)$$

where $r \in (0, 4]$ is the control parameter.

SLIDE: 4

Superstable fixed point (the logistic map)



$$f(x^*, r) = x^*, \quad x^* = x_m, \quad \text{and} \quad f'(x^*, r) = 0 \quad \Rightarrow \quad r = 2. \quad (3)$$

Convergence of x_n about the non-trivial fixed point x^*

$$\eta_{n+1} = \frac{|f''(x^*, r)|}{2!} \eta_n^2 + O(\eta_n^3), \quad (4)$$

is quadratic. The iterates x_n converge quadratically.

D. Kartofelev

YFX1560

4 / 30

In Lecture 9 we showed that the stability of fixed point x^* depends on the absolute slope of f at x^* , i.e., $|f'(x^*)|$. If $|f'(x^*)| < 1$, then the fixed point is stable and for $|f'(x^*)| > 1$ it is unstable.

————— Skip if needed: start —————

Linearisation of a map is derived by studying the slightly perturbed iterate

$$x_n = x^* + \eta_n, \quad (7)$$

where $|\eta| \ll 1$. We study the next iterate dynamics through linearisation of map f

$$\begin{aligned} x_{n+1} = f(x_n) = f(x^* + \eta_n) &= \left[\begin{array}{l} \text{Taylor series ex.} \\ \text{about } x_n = x^* \end{array} \right] = f(x^*) + \frac{f'(x^*)}{1!} (x^* + \eta_n - x^*) + O(\eta_n^2) \approx \\ &\approx x^* + f'(x^*) \eta_n, \end{aligned} \quad (8)$$

$$x_{n+1} = x^* + f'(x^*) \eta_n + O(\eta_n^2), \quad (9)$$

$$\underbrace{x_{n+1} - x^*}_{=\eta_{n+1}} = f'(x^*) \eta_n + O(\eta_n^2). \quad (10)$$

The left-hand side of the result follows from definition (7). The linearised form of map f is obtained by neglecting the higher order terms $O(\eta_n^2)$

$$\boxed{\eta_{n+1} = |f'(x^*)| \eta_n.} \quad (11)$$

————— Skip if needed: stop —————

We know that iterates x_n converge towards stable fixed point x^* where $|f'(x^*)| < 1$ according to the leading term of the Taylor expansion. But what happens for superstable fixed point x^* ? How does the solution converge for $|f'(x^*)| = f'(x^*) = 0$? Obviously, the linearisation can't be used, since the leading term will be zero. We need to include an additional term in the Taylor series expansion:

$$\eta_{n+1} = \underbrace{|f'(x^*)|}_{=0} \eta_n + \frac{|f''(x^*)|}{2!} \eta_n^2 + O(\eta_n^3) = \frac{|f''(x^*)|}{2!} \eta_n^2 + O(\eta_n^3), \quad (12)$$

$$\eta_{n+1} = \frac{|f''(x^*)|}{2!} \eta_n^2 + O(\eta_n^3). \quad (13)$$

This result means that iterates converge **faster than exponentially** when they approach a superstable fixed point. We say that **iterates converge quadratically**. A very beneficial property to keep in mind when analysing maps numerically. A trajectory will require less number of iterates (less calculations) to reach the fixed point—a steady state or equilibrium solution.

The following interactive numerical file demonstrates the superstable or quadratic convergence of iterates x_n in the case of the logistic map given by (6) where $r = 2$.

NUMERICS: NB#1

Comparison of superstable and stable fixed points in the logistic map.

Comparison of map iterate convergence to a superstable fixed point and to a stable fixed point. In the case of superstable fixed point, shown in Fig. 2 (Top), the iterates reach the fixed value in approximately five iterates. In the case of stable fixed points, shown in Fig. 2 (Bottom), the equilibrium point isn't reached even after approximately 20 iterates.

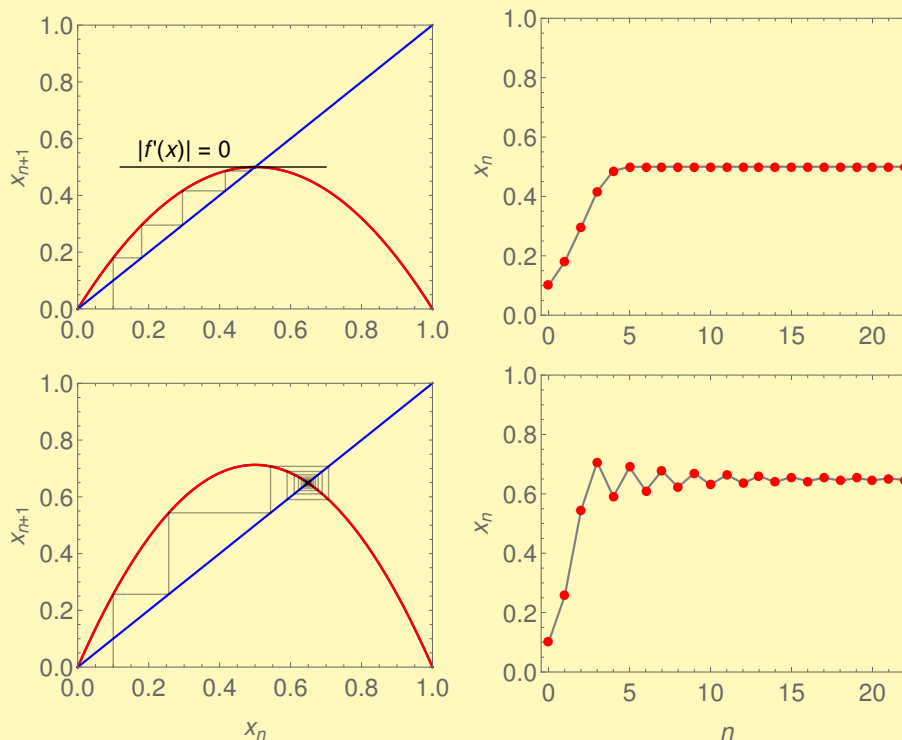
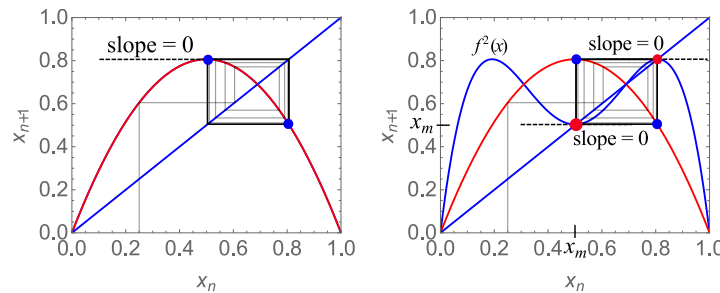


Figure 2: (Top) Cobweb diagram and map iterates of the logistic map featuring a superstable fixed point. The initial condition $x_0 = 0.1$ and the parameter $r = 2$. (Bottom) Cobweb diagram and map iterates of the logistic map featuring a stable fixed point. The initial condition $x_0 = 0.1$ and the parameter $r = 2.85$.

Can there be **superstable period-p points**? Yes there can. The definition is given on the next slide:

Superstable period-p point (the logistic map)

Superstable period-p orbit: $x^* = x_m = \max f$ is also a local min. or max. of f^p map (p-th iterate of map f).



For example in the case of period-2 point

$$f^2(x^*, r) = x^*, \quad (x^* = x_m) \Rightarrow r = 1 + \sqrt{5} \quad (5)$$

$$(f^2(x^*, r))' = \frac{d}{dx^*}[f(f(x^*, r))] = f'(f(x^*, r)) \cdot f'(x^*, r) = 0. \quad (6)$$

D. Kartofelev

YFX1560

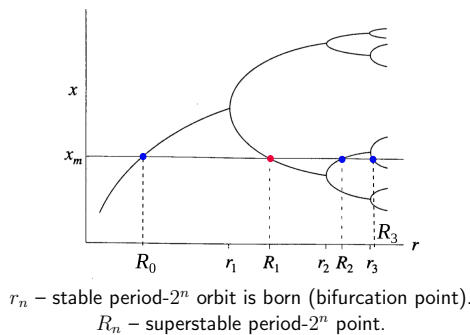
5 / 30

Superstable period-p point: fixed point x^* that is also the local minimum or maximum of map f^p . Algebraically we write

$$f^p(x^*) = x^*, \quad (14)$$

where $x^* = x_m = \max f(x)$. The superstable point of map f where $f(x^*) = x^*$ is also one of the points in the superstable period-p orbit.

Orbit diagram, superstable period- 2^n points



$$\lim_{n \rightarrow \infty} \frac{R_{n-1}}{R_n} = \delta \quad (7)$$

D. Kartofelev

YFX1560

6 / 30

Period doubling bifurcation points

Values of bifurcation points and superstable points of a few first period doublings in the logistic map.

$r_0 = 1.0$ non-trivial	$R_0 = 2.0$	f.p.
$r_1 = 3.0$	$R_1 = 1 + \sqrt{5} \approx 3.23607$	period-2
$r_2 = 1 + \sqrt{6} \approx 3.44949$	$R_2 \approx 3.49856$	period-4
$r_3 \approx 3.54409$	$R_3 \approx 3.55464$	period-8
$r_4 \approx 3.56441$	$R_4 \approx 3.56667$	period-16
$r_5 \approx 3.56875$	$R_5 \approx 3.56924$	period-32
\vdots	\vdots	\vdots
$r_\infty \approx 3.569945672$	$R_\infty = r_\infty \approx 3.56994567$	period- 2^∞

r_∞ – Onset of chaos (accumulation point).

$$\lim_{n \rightarrow \infty} \frac{r_{n-1} - r_{n-2}}{r_n - r_{n-1}} = \lim_{n \rightarrow \infty} \frac{R_{n-1}}{R_n} = \delta \quad (8)$$

D. Kartofelev

YFX1560

7 / 30

The superstable points of the logistic map are shown above on the orbit diagram where r_n is the onset of the period- 2^n orbit (the period doubling or flip bifurcation points) and $r = R_n$ corresponds to superstable period- 2^n orbit. R_n occurs always between r_n and r_{n+1} . Unsurprisingly, the ratios of succeeding R_n also converges to δ for $n \rightarrow \infty$.

1.3 Renormalisation and the Feigenbaum constants

Renormalisation process adds insight into the notion of **the universal route to chaos** presented in the previous lecture. Let's try to tap into the observation, also presented in Lecture 10, that the orbit diagrams of unimodal maps are **self-similar** under magnification or re-scaling. How do the scaling constant α and δ govern the period doubling bifurcations occurring in the logistic and other unimodal maps?

Next, we consider the local dynamics of the orbit diagram near $r = R_0$ and then compare it to the situation near $r = R_1$, see Fig. 3. We **renormalise** one region into another, Region 1 into Region 2 as they appear in Fig. 3. Following slides show graphically what we mean by **renormalisation procedure**.

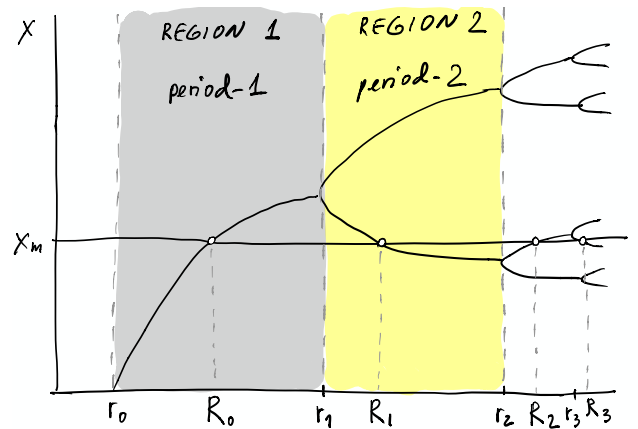
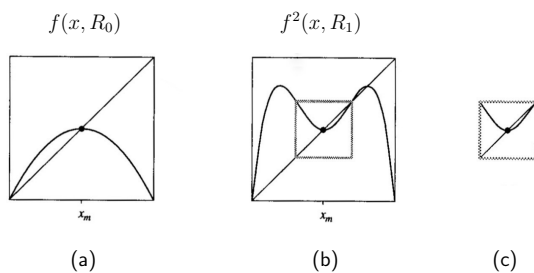


Figure 3: Regions of interest: the proximity to $r = R_0$ and $r = R_1$. Orbit diagram is showing bifurcation points r_n corresponding to the onsets of period- 2^n orbits, and superstable fixed points R_n corresponding to the superstable period- 2^n orbits, cf. Slide 6.

SLIDES: 8, 9

Feigenbaum's analysis, renormalisation

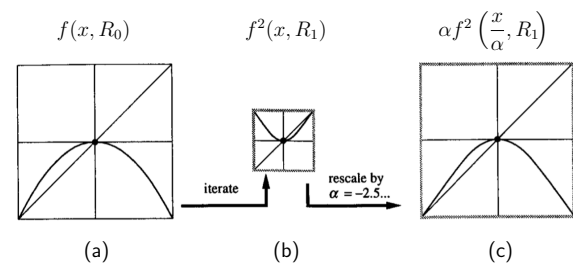


(a)

(b)

(c)

Feigenbaum's analysis, renormalisation



(a)

(b)

(c)

Read: Mitchell J. Feigenbaum, "The universal metric properties of nonlinear transformations," *Journal of Statistical Physics* 21(6), pp. 669–706, 1979. Also relevant to the following three slides ↓.

The visual comparison shows that renormalised map is very similar to the original one. Map maximum x_m shown on Slide 9 has been shifted to the origin in order to simplify the mathematics used below.

Let's express the renormalisation procedure algebraically:

$$f(x, R_0) \approx \alpha f^2\left(\frac{x}{\alpha}, R_1\right), \quad (15)$$

notice that we have scaled the vertical and horizontal directions simultaneously. In summary, map f has been **renormalised** by taking its second iterate (second iterate map), rescaling $x \rightarrow x/\alpha$, shifting r to the next superstable value, and multiplying everything by α .

The higher order renormalisations of $f(x, R_0)$ are given by

$$\begin{aligned} f(x, R_0) &\approx \alpha^2 f^4\left(\frac{x}{\alpha^2}, R_2\right), \\ &\approx \alpha^3 f^8\left(\frac{x}{\alpha^3}, R_3\right), \\ &\approx \alpha^4 f^{16}\left(\frac{x}{\alpha^4}, R_4\right), \\ &\vdots \\ &\approx \alpha^n f^{(2^n)}\left(\frac{x}{\alpha^n}, R_n\right). \end{aligned} \quad (16)$$

What happens when we reach the accumulation point $r = r_\infty$ —reach the chaotic regime? At the limit:

$$\lim_{n \rightarrow \infty} \alpha^n f^{(2^n)}\left(\frac{x}{\alpha^n}, R_n\right) = g_0(x). \quad (17)$$

Feigenbaum found numerically that this limit converges only for $\alpha = -2.502907875\dots$ by producing the resulting limiting function g_0 . The function g_0 is called the **universal limiting function**. This function is similar in shape to map f and it retains the superstability of its fixed point.

The descriptor “**universal**” in this context means that function g_0 is *almost* independent of the initial unimodal map function f . How can g_0 be independent of f ? Function g_0 depends on f only through its behaviour near $x = 0$, since that’s all that survives in the argument x/α^n as $n \rightarrow \infty$. With each renormalisation, we are blowing up smaller and smaller neighbourhoods of the maximum of f until practically all of the information (global shape further away from $x = 0$) of f becomes meaningless. The only remaining information is the **quadratic** nature of the maximum. In the case of unimodal maps the Taylor expansion at $x^* = x_m$ has to have the second (quadratic) x^2 term (superstability). The fixed point has to be what is called the **second degree maximum** point or the **quadratic** maximum.

You can find the universal limiting functions related to any superstable period- 2^i orbit. To obtain other universal limiting functions $g_i(x)$, start with $f(x, R_i)$ instead of $f(x, R_0)$:

$$g_i(x) = \lim_{n \rightarrow \infty} \alpha^n f^{(2^n)}\left(\frac{x}{\alpha^n}, R_{n+i}\right). \quad (18)$$

What happens at the onset of chaos where $i = \infty$? Let’s find the universal limiting function at the onset of chaos where $R_i = R_\infty$. We need to renormalise $f(x, R_\infty)$ one time

$$g_\infty(x) \approx \alpha f^2\left(\frac{x}{\alpha}, R_{\infty+1}\right) = \left[\begin{array}{l} \text{Reminder:} \\ \infty + 1 = \infty \end{array} \right] = \alpha f^2\left(\frac{x}{\alpha}, R_\infty\right) = g(x). \quad (19)$$

For once, we don’t have to shift r when we renormalise in other words we became independent of $r = R_i$! The limiting function $g_\infty(x)$, usually called simply $g(x)$, satisfies the following equation:

$$g_\infty(x) = \alpha g_\infty^2\left(\frac{x}{\alpha}\right) \Rightarrow \boxed{g(x) = \alpha g^2\left(\frac{x}{\alpha}\right)}. \quad (20)$$

This is a **functional equation** for $g(x)$ and the universal scale factor α . It is **self-referential**: primary unknown $g(x)$ is defined in terms of itself.

Let’s try to solve Eq. (20). The functional equation is not complete until we specify boundary conditions on $g(x)$. After the shift of origin, all our unimodal f ’s have a maximum at $x = 0$, so we require

$$g'(0) = 0. \quad (21)$$

Also, we can set

$$g(0) = \left[\begin{array}{l} \text{From Def. (19)} \\ \text{we know that} \end{array} \right] = g(0, R_\infty) = \text{const.}, \quad (22)$$

to

$$g(0) = 1, \quad (23)$$

without loss of generality. This just defines the normalised scale for x ; if $g(x)$ is a solution of Eq. (20), so is $\mu g(x/\mu)$ where $\mu \in \mathbb{R}$, with the same μ . Naturally, this selection agrees with boundary condition (21).

Now we can solve Eq. (20) for function $g(x)$ and α at the boundary $x = 0$:

$$g(0) = \alpha g^2\left(\frac{0}{\alpha}\right) = \alpha g^2(0) = \alpha g(g(0)), \quad (24)$$

since $g(0) = 1$ we have

$$1 = \alpha g(1), \quad (25)$$

$$\boxed{\alpha = \frac{1}{g(1)}}. \quad (26)$$

The universal scaling constant α depends on the limiting function g . As of now no closed form solution exists for function g . We can resort to numerical method to find the shape of the limiting function g and the value of α . Next, we solve Eq. (20) with boundary condition (26) using power series expansion:

1.4 Numerical determination of the Feigenbaum α constant

SLIDES: 10, 11

Limiting function $g(x)$ and Feigenbaum constant α

Let's consider a functional equation in the following form:

$$g(x) = \alpha g\left(g\left(\frac{x}{\alpha}\right)\right) = \alpha g^2\left(\frac{x}{\alpha}\right), \quad (9)$$

where α acts as a scaling coefficient and

$$\alpha = \frac{1}{g(1)}. \quad (10)$$

The power series solution is obtained by assuming a power expansion in the following form:

$$g(x) = 1 + ax^2 + bx^4 + cx^6 + dx^8 + ex^{10} + \dots, \quad (11)$$

where the map maximum is quadratic.

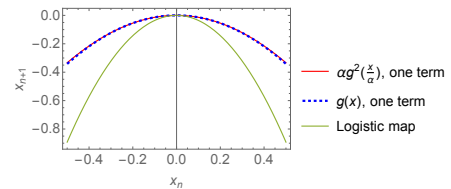
Limiting function $g(x)$ and Feigenbaum constant α

Numeric solution¹: The one term approximation where

$$g(x) = 1 + ax^2 + O(x^4), \quad (12)$$

results in

$$a = -\frac{1}{2}(1 + \sqrt{3}), \quad \alpha = \frac{1}{g(1)} \approx -2.73205, \quad (9.2\% \text{ error}). \quad (13)$$



¹See Mathematica .nb file uploaded to the course webpage.

The power series expansion uses the Maclaurin expansion and assumes a **quadratic maximum**. The quadratic maximum follows from the superstability property. The above process can generate lots of extraneous roots you will need to shift through them to find the correct solution.

The solution shown above is taken from the following numerical file. The file is commented for the benefit of students who are interested in numerical methods in general.

NUMERICS: NB#2

Calculation of universal limiting function g and value of the Feigenbaum constant α in the case of the logistic map using power series expansion: one and four term approximations.

In order to find a better match more terms in the power series expansion are needed:

SLIDE: 12

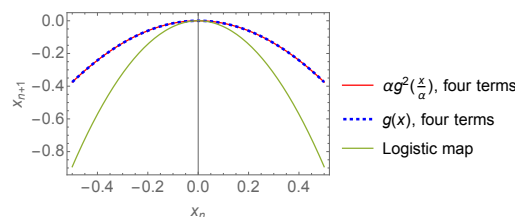
Limiting function $g(x)$ and Feigenbaum constant α

Numeric solution²: The four term approximation where

$$g(x) = 1 + ax^2 + bx^4 + cx^6 + dx^8 + O(x^{10}). \quad (14)$$

Coefficients: $a \approx -1.528$, $b \approx 0.1053$, $c \approx 0.02631$, $d \approx -0.003344$ and

$$\alpha = \frac{1}{g(1)} \approx -2.50316, \quad (0.01\% \text{ error}). \quad (15)$$



²See Mathematica .nb file uploaded to the course webpage.

The solution shown above is taken from the following numerical file.

NUMERICS: NB#2

Calculation of universal limiting function g and value of the Feigenbaum constant α in the case of the logistic map using power series expansion: one and four term approximations.

The renormalisation theory also explains the value of δ . Unfortunately, the derivations and analysis of the Feigenbaum δ constant requires advanced functional analysis know-how (operators in function space, the Frechet derivatives, etc.) and for this reason is omitted from this course.

Note: Something qualitative (unimodality) gave us something quantitative (the Feigenbaum constants). In science it is usually the other way around!

Reading suggestion

Link	File name	Citation
Paper#1	paper5.pdf	Mitchell J. Feigenbaum, “The universal metric properties of nonlinear transformations,” <i>Journal of Statistical Physics</i> , 21 (6), pp. 669–706, (1979). doi:10.1007/BF01107909

2 Discrete-time analysis methods

We have already used mapping procedure to map a continuous 3-D flow into a discrete 1-D map—the Lorenz attractor \rightarrow the Lorenz map. Our goal in this section is to generalise this approach.

2.1 The Poincaré section and the Poincaré map

The **Poincaré section** is a set of intersection points between an $n - 1$ dimensional hyperspace, hyper-surface, or hyperplane and a trajectory of n -dimensional continuous-time flow. The **Poincaré map or return map** is the (algebraic) relationship between these preceding and succeeding intersection points, i.e., point \vec{x}_k and \vec{x}_{k+1} , where k denotes the index of the intersection point found on a Poincaré section, see Slides 13 and 14.

The **Poincaré maps** are useful for studying swirling flows, such as the flow near a periodic orbit or as we’ll see later, the flow in some chaotic systems. Consider an n -dimensional system:

$$\dot{\vec{x}} = \vec{f}(\vec{x}). \quad (27)$$

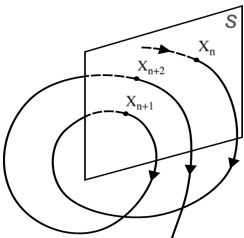
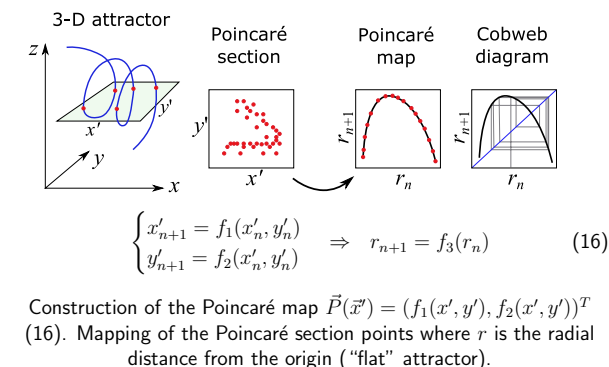
Let S be an $n - 1$ dimensional surface, see Slide 13. Surface S is required to be transverse to the flow, i.e., all trajectories starting on S flow through it, not parallel to it. The Poincaré map \vec{P} is a mapping from S to itself, obtained by following trajectories from one intersection with S to the next. If $\vec{x}_k \in S$ denotes the k -th intersection, then the Poincaré map is defined by

$$\vec{x}_{k+1} = \vec{P}(\vec{x}_k). \quad (28)$$

Suppose that \vec{x}^* is a fixed point of \vec{P} , i.e., $\vec{P}(\vec{x}^*) = \vec{x}^*$. Then a trajectory starting at \vec{x}^* returns to \vec{x}^* after some time t , and is therefore a closed orbit for the original system (27). Moreover, by looking at the behaviour of \vec{P} near this fixed point, we can determine the stability of the closed orbit.

Thus the Poincaré map converts problems about closed orbits (which are difficult) into problems about fixed points of a mapping (which are easier in principle, though not always in practice). The snag is that it’s typically impossible to find a formula for \vec{P} .

SLIDES: 13–16

The Poincaré section	Discrete-time dynamics analysis
 <p style="text-align: center;">Intersection of an attractor trajectory with hypersurface S.</p>	 <p style="text-align: center;">Construction of the Poincaré map $\vec{P}(\vec{x}) = (f_1(x', y'), f_2(x', y'))^T$ (16). Mapping of the Poincaré section points where r is the radial distance from the origin (“flat” attractor).</p>
D. Kartofelev YFX1560 13 / 30	D. Kartofelev YFX1560 14 / 30

2.1.1 Example of finding a Poincaré map formula

For the sake of illustration, we present an examples for which the Poincaré map \vec{P} can be computed explicitly. Consider the vector field given in polar coordinates by

$$\begin{aligned}\dot{r} &= r(1 - r^2), \\ \dot{\theta} &= 1.\end{aligned}\tag{29}$$

This decoupled system is familiar to us. We analysed it in Lecture 6. Angular velocity $\dot{\theta}$ is constant and positive. The behaviour of a trajectory in the radial direction is described by the first equation. 1-D phase portrait of the first equation is shown in Fig. 4. We can sketch the phase portrait corresponding to Sys. (29) by combining the above observations. Figure 5 shows the resulting phase portrait and the stable limit-cycle associated with the fixed point $r^* = 1$ of the first equation present in Sys. (29).

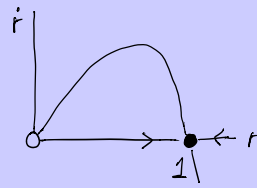


Figure 4: Phase portrait of the 1-D equation featured in (29) where the stable fixed point $r^* = 1$.

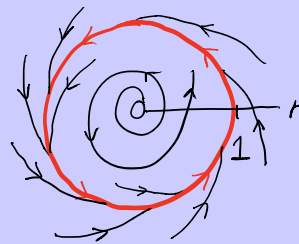


Figure 5: Phase portrait shown in polar coordinates corresponding to Sys. (29). Stable limit-cycle is shown with the red closed trajectory.

Let S be the positive x -axis that also coincides with the r -axis in polar coordinate representation. Compute the Poincaré map. Show that the system has a unique and stable periodic orbit defined by the stable limit-cycle shown above.

Solution: Let r_0 be an initial condition on S . Since $\dot{\theta} = 1$, the first return to S occurs after a **time of flight** $t = 2\pi$. Then $r_1 = P(r_0)$, where r_1 satisfies:

$$\frac{dr}{dt} = r(1 - r^2),\tag{30}$$

$$dt = \frac{dr}{r(1 - r^2)},\tag{31}$$

$$\int_{r_0}^{r_1} \frac{dr}{r(1 - r^2)} = \int_0^{2\pi} dt = 2\pi,\tag{32}$$

$$\int_{r_0}^{r_1} \frac{dr}{r(1 - r^2)} = 2\pi.\tag{33}$$

Evaluation of the integral and solving for r_1 yields:

$$r_1 = [1 + e^{-4\pi}(r_0^{-2} - 1)]^{-1/2}.\tag{34}$$

Hence, the sought map formula:

$$P(r) = [1 + e^{-4\pi}(r^{-2} - 1)]^{-1/2}, \quad (35)$$

and the Poincaré map takes the following form:

$$r_{n+1} = P(r_n) = [1 + e^{-4\pi}(r_n^{-2} - 1)]^{-1/2}. \quad (36)$$

The graph of P and the cobweb diagram for r_0 is plotted in Fig.6. The cobweb diagram shows that the fixed point $r^* = 1$ is stable and unique. No surprise, since we knew from above that this system has a stable limit-cycle at $r = 1$.

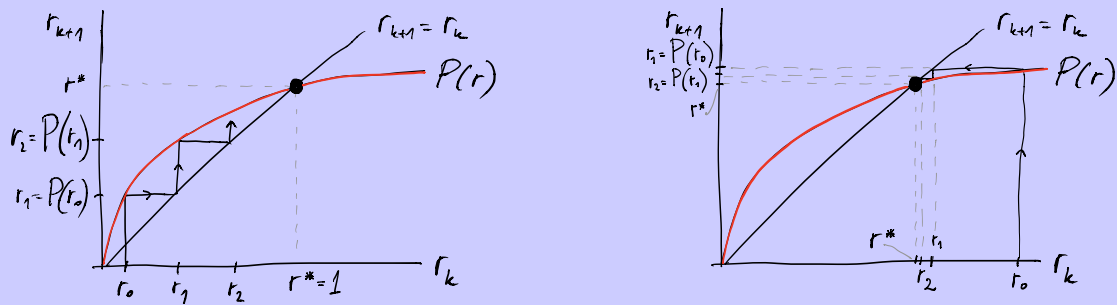
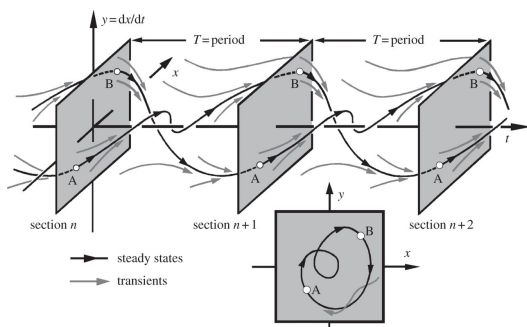


Figure 6: (Left) Cobweb diagram of the found Poincaré map where initial condition $r_0 \lesssim r^* = 1$. (Right) Cobweb diagram where initial condition $r_0 \gtrsim r^* = 1$.

The Poincaré section, periodic forcing³



³Credit: J. Thompson, H. Stewart, 1986, *Nonlinear dynamics and chaos: geometrical methods for engineers and scientists*. Chichester, UK: Wiley.

D. Kartofelev

YFX1560

15 / 30

The Poincaré section, periodic forcing

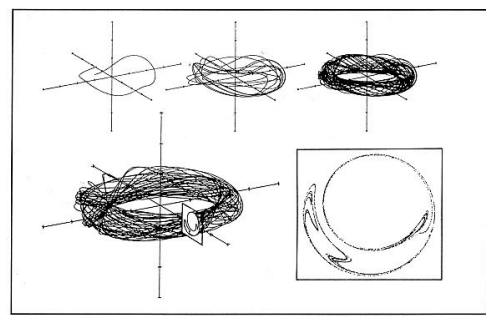


Figure 3. Illustration of a Strange Attractor and the Associated Poincaré Map (from James Gleick, *Chaos: Making a New Science* [New York: Penguin Books 1987], 143)

D. Kartofelev

YFX1560

16 / 30

Slides 15 and 16 show two additional ways of visualising the Poincaré sections. These ideas are expanded below.

Note (from Lecture 9): The Poincaré mapping is not the same as the Lorenz mapping discussed in Lecture 9. In both cases we're trying to simplify the analysis of a differential equation by reducing it to an iterated map of some kind. But there's an important distinction: To construct a Poincaré map for a three-dimensional flow, we compute a trajectory's successive intersections with a two-dimensional surface. The Poincaré map takes a point on that surface, specified by two coordinates, and then tells us how those two coordinates change after the first return to the surface. The Lorenz map is different because it characterises the trajectory by only one number, not two. This simpler approach works only if the attractor is very "flat," i.e., close to two-dimensional, as the Lorenz attractor is.

2.2 The Poincaré analysis of the periodically driven damped Duffing oscillator

The Duffing equation or the Duffing oscillator, named after Georg Duffing (1861–1944), is a nonlinear second-order differential equation used to model certain damped and driven oscillators. The next slides

introduce this system:

SLIDES: 17, 18

The first term on the left-hand side of Eq. (17) on Slide 17 is the inertial term, the third term is the nonlinear stiffness, and the fourth term is the damping. The **non-homogeneous** right-hand side of the equation describes the external 2π -periodic forcing with amplitude F and frequency $\omega = 1$. The solution for $F > 0$ may be a **strange attractor**. The external forcing of two-dimensional systems is often the source of chaos. But wait, how can two-dimensional system feature chaos? Isn't chaos supposed to be reserved only for three or higher-dimensional systems. The *external* forcing term allows for this second order system to be represented as a three-dimensional system:

The periodically driven damped Duffing oscillator

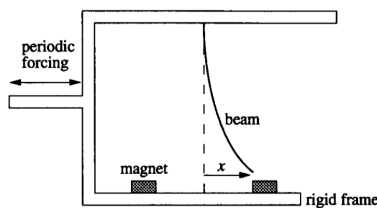


Figure: The mechanical Duffing oscillator.

The non-autonomous equation of motion has the following form:

$$\ddot{x} - x + x^3 + \delta \dot{x} = F \cos \omega t, \quad (17)$$

where δ is the damping coefficient, F and ω are the forcing strength and frequency, respectively.

D. Kartofelev

YFX1560

17 / 30

The periodically driven damped Duffing oscillator

We introduce the variable exchange $y = \dot{x}$ and rewrite (17)

$$\begin{cases} \dot{x} = y, \\ \dot{y} = x - x^3 - \delta y + F \cos \omega t. \end{cases} \quad (18)$$

The equivalent 3-D system is obtained by applying variable exchange $z = \omega t$

$$\begin{cases} \dot{x} = y, \\ \dot{y} = x - x^3 - \delta y + F \cos z, \\ \dot{z} = \omega. \end{cases} \quad (19)$$

The above holds since

$$z = \int \dot{z} dt = \int \omega dt = \omega \int dt = \omega t + C. \quad (20)$$

D. Kartofelev

YFX1560

18 / 30

Note: If you remove the damping and the *external* forcing terms the system becomes equivalent to the problem of a particle in a double-well potential given by the following potential function:

$$V(x) = \frac{x^4}{4} - \frac{x^2}{2}, \quad (37)$$

this potential was presented and studied in Lecture 5.

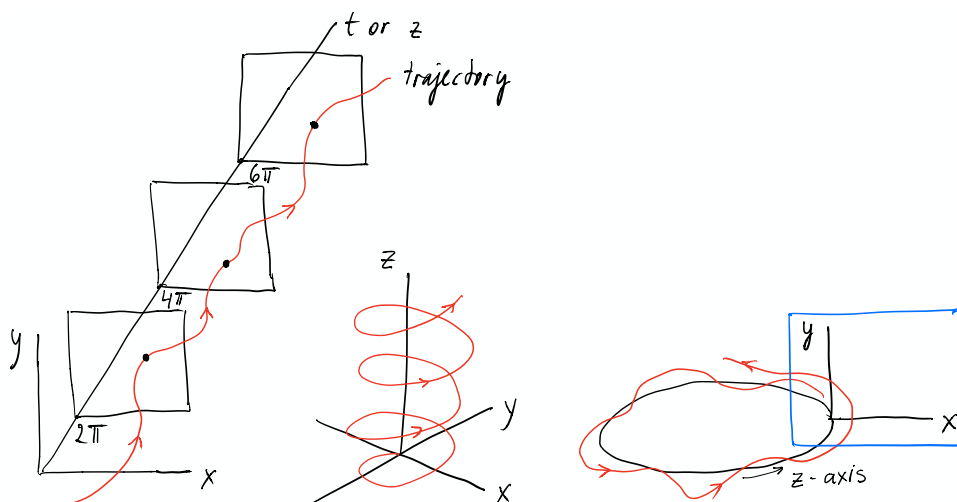


Figure 7: (Left) Snapshots of a trajectory every 2π time units (time of flight, assuming $\omega = 1$), cf. Slide 15. The 2π -periodicity is a natural choice since the external force is 2π -periodic for $\omega = 1$. (Middle) A trajectory in the three-dimensional Cartesian xyz -space corresponding to Sys. (18) shown on Slide 18. (Right) A trajectory in the three-dimensional space where the z -axis is 2π -periodic and is folded into a closed circle, cf. Slide 16. The blue outline shows the Poincaré section.

Figure 7 shows three ways you can think graphically about the solution trajectories of the Duffing oscillator and its Poincaré section *cf.* NB#3, Slides 15 and 16. Below we assume that in the external forcing term $\omega = 1$. The following numerical file shows the solution to Duffing oscillator, and the quantitatively accurate renderings of the three different ways to plot trajectories of the Duffing oscillator shows in Fig. 7.

NUMERICS: NB#3

The periodically forced damped Duffing oscillator: numerical solution and a phase portrait. The 2π -periodic Poincaré section of the Duffing oscillator (static).

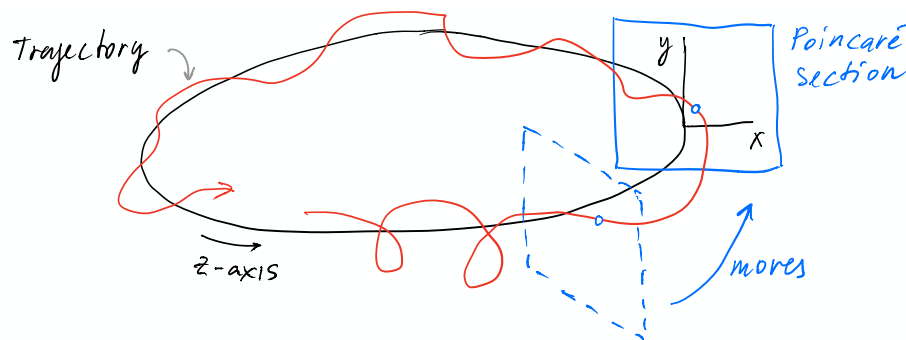
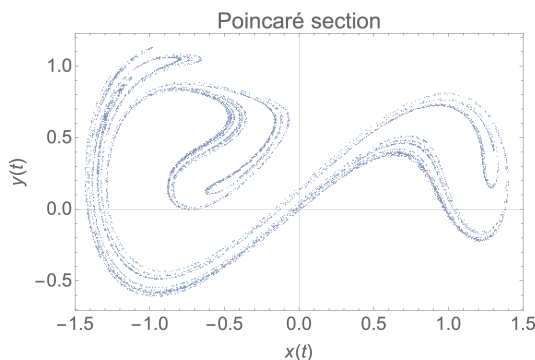


Figure 8: Poincaré section dynamics and periodic z -axis. A moving Poincaré section featuring a single intersection point shown with the blue bullet. There is one intersection point because the integration time $t \ll 1$. The section moves in the direction of the blue arrow along the closed z -axis.

The following slides show how the Poincaré section of the Duffing oscillator calculated for prolonged integration time, i.e., $t \gg 1$ changes as we continuously move it along the 2π -periodic time or z -axis as shown in Fig. 8.

SLIDES: 19, 20

The Poincaré section⁴ of the Duffing oscillator



⁴See Mathematica .nb file uploaded to the course webpage.

The Poincaré section dynamics: Duffing oscillator



No embedded video files in this pdf

Notice that the Poincaré section is depicting something that can be described as continuous **stretching**, **folding** and **re-injection** of the initial cloud of intersection points into itself. A careful visual inspection of the intersection points will reveal that they are being progressively **mixed**, within the region defined by the attractor, by this **stretching–folding–re-injection** process. This type of **Poincaré section dynamics** is common for strange attractors.

The dynamics of the Poincaré section of the Duffing oscillator is explored in the following numerical file.

NUMERICS: NB#4

The periodically forced damped Duffing oscillator and a dynamic animation of the Poincaré section.

2.3 The Poincaré analysis of the Rössler attractor

The Rössler attractor was originally proposed and studied by Otto Rössler (1940–). The system is a product of pure imagination and it exhibits chaotic dynamics by design.

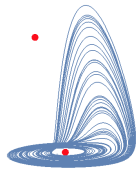
SLIDES: 21–26

The Rössler attractor

As mentioned in Lecture 9 the Rössler attractor⁵ is given by:

$$\begin{cases} \dot{x} = -y - x, \\ \dot{y} = x + ay, \\ \dot{z} = b + z(x - c). \end{cases} \quad (21)$$

Chaotic solution exists for $a = 0.1$, $b = 0.1$, $c = 14$.



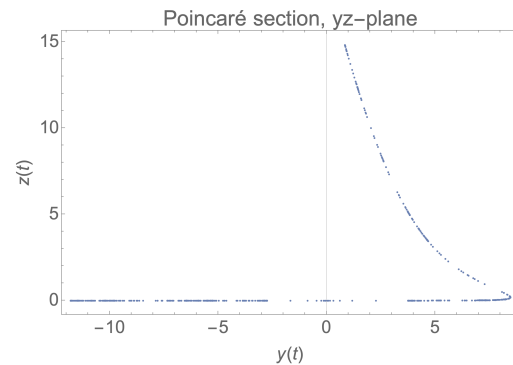
⁵See Mathematica .nb file uploaded to the course webpage.

D. Kartofelev

YFX1560

21 / 30

The Rössler attractor: the Poincaré sections⁶



⁶See Mathematica .nb file uploaded to the course webpage.

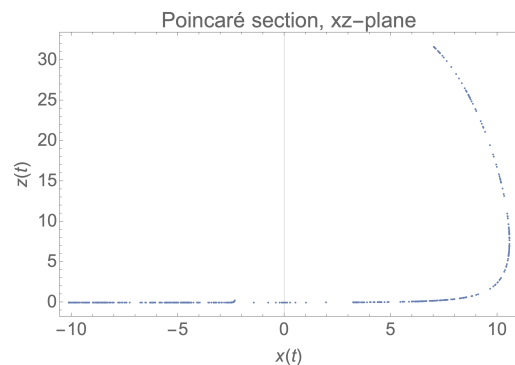
D. Kartofelev

YFX1560

22 / 30

The system has only one nonlinearity the zx term in the third equation.

The Rössler attractor: the Poincaré sections⁷



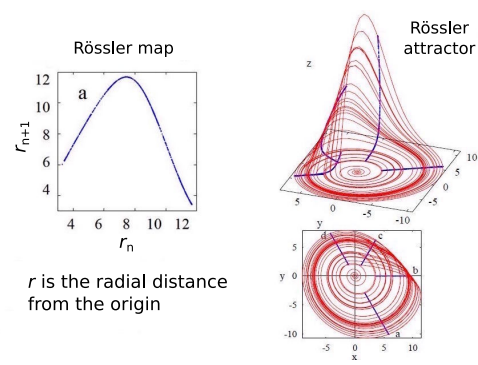
⁷See Mathematica .nb file uploaded to the course webpage.

D. Kartofelev

YFX1560

23 / 30

Rössler system: return map and Poincaré sections



Credit: Y. Maistrenko and R. Paškauskas

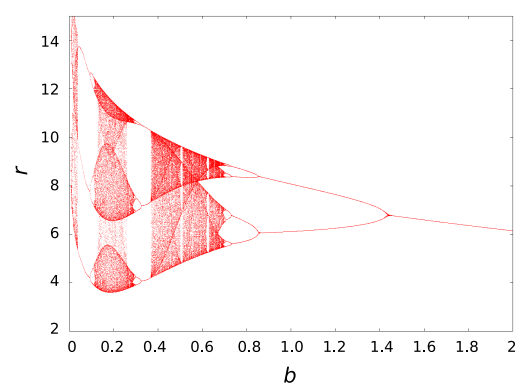
D. Kartofelev

YFX1560

24 / 30

Slide 24 features the numerically calculated shape of the Rössler map—the Poincaré map of the Rössler attractor given in polar coordinates.

The Rössler attractor: an orbit diagram



D. Kartofelev

YFX1560

25 / 30

The Rössler attractor: period doubling



No embedded video files in this pdf

D. Kartofelev

YFX1560

26 / 30

The orbit diagram shown on Slide 25 is calculated using the Rössler map, shown on Slide 24. It clearly features period doubling bifurcations and chaotic regions with periodic window bands in it, just like the logistic and sine maps do. Slide 26 shows the period doubling happening in the time-integrated solution.

The following numerical file was used to calculate the attractor and the Poincaré sections shown above.

NUMERICS: NB#5

Numerical solution of the Rössler attractor. The Poincaré section of the Rössler attractor.

The following interactive numerical file shows the period doubling bifurcation happening in the xy -projection of the Rössler attractor, cf. Slides 25 and 26.

NUMERICS: NB#6

Periodic orbits in the Rössler attractor for varied c value.

The following slide shows the 2π -periodic dynamics of the Poincaré section of the Rössler attractor.

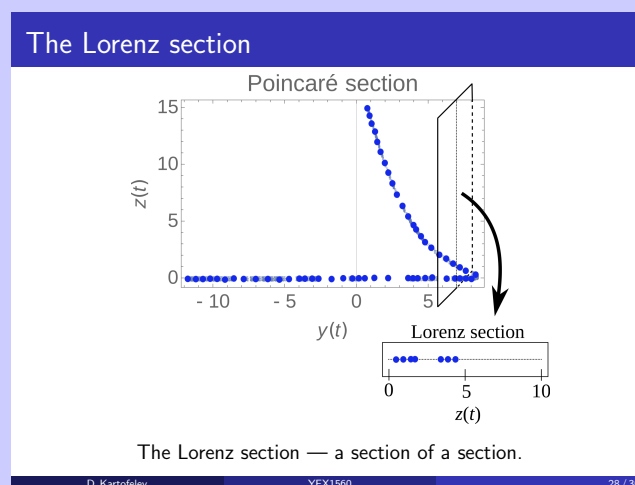
SLIDE: 27



Once again, notice the **folding, stretching and re-injection**, and consequent **mixing** of the Poincaré section points, cf. Slides 19 and 20. This type of Poincaré section dynamics will be explored further in the next week's lecture.

3 The Lorenz section of 3-D attractors

SLIDE: 28



The above slide shows a two-dimensional Poincaré section of a strange attractor where we sliced the attractor with a perpendicular plane, thereby exposing its cross section. Here, we assume that the

attractor is shown for $t \gg 1$. If we take a further one-dimensional slice or the **Lorenz section** through the Poincaré section, we find an infinite set of points separated by gaps of various sizes. In the next week's lecture we will look into this object and into the notion of the Lorenz section in greater detail.

4 Attractor reconstruction

In applications it is often the case that you are able to measure or are restricted to only measuring one time-series related to a higher order system—one aspect of a problem, one variable. Let's say you need to analyse the attractor that governs your measured one-dimensional time-series signal $s(t)$, e.g., show that it is strange. At first it might seem that there is not enough information. But, there exists a surprising data analysis technique known as the **attractor reconstruction**.

For systems governed by an attractor, the dynamics in the full higher dimensional phase space can be reconstructed from measurements of just a single time series $s(t)$! A single variable carries sufficient information about all the others. The method is based on time delays τ . For instance, define a two-dimensional vector

$$\vec{x}(t) = (s(t), s(t + \tau))^T, \quad (38)$$

for some time delay $\tau > 0$ and signal $s(t)$ where $\vec{x} = (x, y)^T$. Signal $s(t)$ can therefore represent either the variable $x(t)$ or $y(t)$. The time-series $s(t)$ generates a trajectory $\vec{x}(t)$ in a two-dimensional phase space that represents its attractor's trajectory. You can also consider the attractor in three dimensions, by defining the three-dimensional vector

$$\vec{x}(t) = (s(t), s(t + \tau), s(t + 2\tau))^T, \quad (39)$$

for time delay $\tau > 0$. For four-dimensional attractor use $\vec{x}(t) = (s(t), s(t + \tau), s(t + 2\tau), s(t + 3\tau))^T$, etc.

The following interactive numerical file demonstrates attractor reconstruction using three examples. First, a sine wave is used to reconstruct its two-dimensional attractor—a circle. Second, a quasi-periodic signal is used to reconstruct its three-dimensional attractor—a surface of a torus. Third, time-series $x(t)$, $y(t)$ and $z(t)$ of the Lorenz system are used to reconstruct the three-dimensional Lorenz attractor.

NUMERICS: NB#7

Higher-dimensional attractor reconstruction from 1-D time-domain signals. Examples: a sine wave, a quasi-periodic signal, and all three variables $x(t)$, $y(t)$ and $z(t)$ of the Lorenz attractor calculated for the *usual* chaotic parameter values.

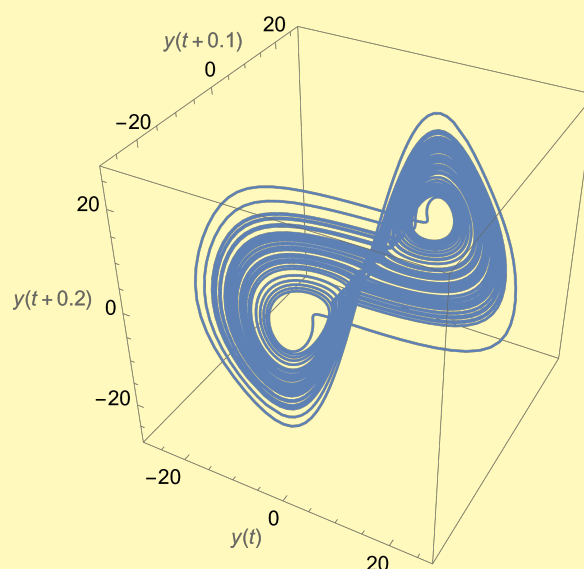


Figure 9: Reconstructed three-dimensional Lorenz flow using only the time-series $y(t)$. Time series $y(t)$ is calculated from the Lorenz system for parameter values $d = 10$, $r = 28$ and $b = 8/3$ and for initial condition $(x(0), y(0), z(0)) = (6, 6, 10)$.

Figure 9 show a reconstruction of the Lorenz attractor.

Revision questions

1. What are the values of the Feigenbaum constants?
2. What are the Feigenbaum constants (more in-depth answer)?
3. Define superstable fixed point of a map.
4. Define superstable period-p point (or period-p orbit) of a map.
5. What are the universals of unimodal maps?
6. What is the universal route to chaos?
7. Idea behind renormalisation?
8. What are the universal limiting functions in the context of maps?
9. Name discrete-time dynamics analysis methods.
10. What is the Poincaré section?
11. What is the Poincaré map (return map)?
12. What is the Lorenz section?